Applying a joint geophysical inversion approach for medical imaging

Jie Zhang, Ziang Li, Dong Liu, and Jiangfeng Du, University of Science and Technology of China (USTC)*

Summary

We present a computed tomography (CT) image-guided electrical impedance tomography (EIT) method for medical imaging by applying a joint geophysical inversion approach. CT is a robust medical imaging modality for accurately reconstructing the density structure of the region being scanned. EIT can detect electrical impedance abnormalities to which CT scans may be insensitive, but the poor spatial resolution of EIT is a major concern for medical applications. In this study, we develop a CT image-guided EIT (CEIT) based on the cross-gradient method. We assume that both CT scanning and EIT imaging are conducted for the same medical target. A CT scan is first acquired to help solve the subsequent EIT imaging problem. During EIT imaging, we apply cross gradients between the CT image and the electrical conductivity distribution to iteratively constrain the conductivity inversion. The cross-gradient based method allows the mutual structures of different physical models to be referenced without directly affecting the polarity and amplitude of each model during the inversion. We apply the CEIT method to both numerical simulations and phantom experiments. The results show that the CEIT method can significantly improve the quality of conductivity images.

Introduction

It is essential to create visual representations of the interior of the human body for clinical analysis and medical intervention. Each of the various existing medical imaging technologies generally measures different types of data and presents images associated with different physiological properties of the structures, organs, and tissues of the human body. The need to combine morphologic and functional information has motivated the development of multimodality imaging in the field of diagnostic imaging (Martí-Bonmatí et al., 2010). This scenario is similar to geophysical imaging employed to delineate oil and gas reservoirs in the earth; however, the geological scale is much larger than the human body. Seismic waves are sensitive to the interfaces between rock formations, but only the electrical properties are significantly different across the interface between oil and water (Zhang and Morgan, 1997). The oil and gas industry has transitioned from single-modality geophysical imaging to joint multi-physical imaging, in which multiple geophysical datasets are processed simultaneously with the application of mutual constraints (Gallardo and Meju, 2003; 2004; Colombo and Stefano, 2007).

The challenge with multiple datasets is similar in both medical and geophysical imaging: how can different imaging processes dealing with entirely different physical properties of the same target be incorporated to affect one another? In 2003, two geophysicists in the UK, Luis Alonso Gallardo and Maxwell Azuka Meju, developed a novel technology that allows multiple imaging processes accounting for different properties of the same target to influence one another simultaneously by imposing cross gradients between two different models (Gallardo and Meju, 2003; 2004). More than 570 technical papers by researchers worldwide have been published following their approach investigating ways to solve various joint geophysical imaging problems. In 2019, Gallardo and Meju received the Reginald Fessenden Award from the Society of Exploration Geophysicists (SEG) for their breakthrough invention. In this study, we extend the cross-gradient technology developed by Gallardo and Meju for the field of oil and gas exploration to medical imaging with the specific intent of developing CT-guided electrical impedance tomography (Li et al., 2020).

The advent of CT has revolutionized diagnostic radiology (Brenner and Hall, 2007; Histed et al., 2012). CT is a structural imaging technology with a high spatial resolution. EIT is a relatively new technique in the field intended for noninvasively imaging the electrical conductivity or resistivity distribution within a human body (Webster, 1990). Animal and clinical studies have revealed that many diseases, such as cardiac arrhythmias, osteoporosis, and leukemia (Chen et al., 2004; Balmer et al., 2018), are associated with electrical conductivity abnormalities. To date, this imaging approach has shown satisfactory results in certain functional imaging studies and may offer a certain advantage in tumor analysis compared with CT. However, EIT is not yet fully suitable for anatomical imaging due to its poor spatial resolution (Chitturi et al., 2017).

Resistivity forward modeling and inversion

In the medical EIT imaging problem, the forward and inverse problem is very similar to the geophysical *d.c.* resistivity imaging problem, except for boundary conditions imposed for human body. The EIT imaging problem begins with forward modeling. The forward problem that aims to obtain the voltage response caused by the injection of current is solved by a finite-element method in this study. We demonstrate the problem by a 2D problem and solution, but the approach is applicable to 3D human body as well.

Joint inversion for medical imaging

The potential $\varphi(x,y)$ in the domain Ω can be modeled by the generalized Laplace equation:

$$\nabla \cdot (\sigma(x,y)\nabla\varphi(x,y)) = 0, \quad (x,y) \in \Omega, \tag{1}$$

where $\sigma(x,y)$ is the conductivity distribution function.
The boundary conditions are as follows

$$\varphi(x,y) + z_l \sigma(x,y) \frac{\partial \varphi(x,y)}{\partial n} = U_l, \ (x,y) \in e_l, \tag{2}$$

$$\sigma(x,y) \frac{\partial \varphi(x,y)}{\partial n} = 0, \ (x,y) \in \partial\Omega \setminus \bigcup_{l=1}^{L} e_l, \tag{3}$$

where z_l is the contact impedance between the electrodes and the imaged body, n represents the unit vector of the outward normal direction on the boundary of the measurement area, U_l is the potential at the electrode e_l, $\partial\Omega$ denotes the boundary of the 2D measurement area, and l=1,2,…, L is the number of electrodes.

The objective function for inversion is defined by:

$$F(\mathbf{m}_E) = \left\|\mathbf{d}_E - S(\mathbf{m}_E)\right\|^2 + \left\|\alpha \mathbf{L}\mathbf{m}_E\right\|^2 + \left\|\beta t(\mathbf{m}_E, \mathbf{m}_C)\right\|^2 \tag{4}$$

where β represents the cross-gradient coefficient and $t(m_E,m_C)$ is the 2D cross gradient vector term between the conductivity m_E and the CT value m_C.

The cross-gradient function is given by

$$t(\mathbf{m}_E, \mathbf{m}_C) = \nabla \mathbf{m}_E(x,y) \times \nabla \mathbf{m}_C(x,y). \tag{5}$$

The above cross-gradient function between two different physical properties follows the joint geophysical inversion method defined by Gallardo and Meju (2003, 2004).

For electrical impedance measurements for human body, there are a few standard recording geometries. A PXI-based EIT recording geometry (Kuopio Impedance Tomography 4 (KIT4)) (Kourunen et al., 2008) is applied. The KIT4 recording geometry consists of 16 electrodes, 4 of which are sink electrodes {1, 5, 9, 13}. The injections are carried out pairwise between one sink electrode and the other 15 electrodes, leading to a total of 54 injections when reciprocal injections are removed.

Numerical examples

We conduct numerical imaging of a simple blocky model that simulates the human thorax (Fig. 1). Three polygons are distributed within a circular boundary with a diameter of 2 cm. The background is homogenous. The analyses in this section involve noise-free data and address the issues of parameter selection, target shape error, and insufficient information in the reference CT image. We shall test a few numerical models with lung and heart simulation.

In the numerical simulations, the measurement data are obtained by solving the forward problem described above. The injected current is set to 1 A with a frequency of 10 kHz. Sixteen electrodes with a length of 0.22 cm are attached to the boundary of the target. The contact impedance is set to 1×10^{-4} $\Omega\cdot m^2$ for all electrodes.

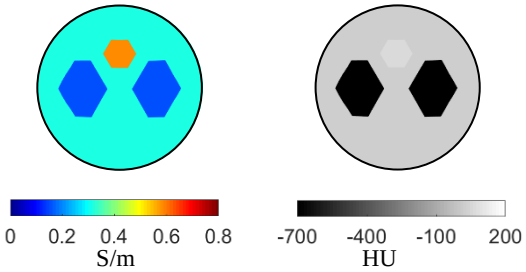

Fig 1: A blocky distribution. (a) True EIT model; b) the CT scan.

The simulated conductivity and CT value distributions are shown in Fig. 1. The conductivities of the inclusions are set to 0.15 S/m for the two 'lung' objects, 0.6 S/m for the 'heart' object and 0.33 S/m for the 2D model background, corresponding to values found in the literature (Gabriel et al., 2009). The CT values are set to -700 HU, 60 HU, and 30 HU for the 'lungs', 'heart', and background, respectively.

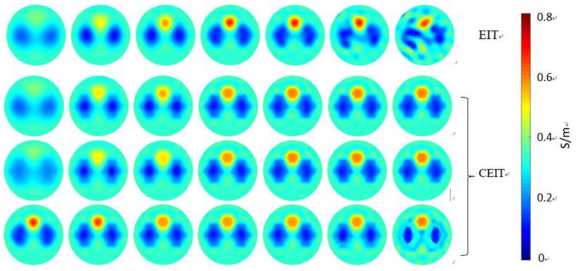

Fig 2: Reconstructed images with different choices of α and β by using tomography with or without CT constraint.

Appropriate scaling factors are important for obtaining accurate tomography results. For EIT, the regularization parameter α controls the trade-offs between the voltage error and the Tikhonov regularization term. On the other hand, the parameters α and β in CEIT control the trade-offs among the data misfit, the Tikhonov regularization term, and the cross-gradient function term. A series of scaling factors are tested in this study. Some of the results of the reconstruction are shown in Fig. 2. The first row of Fig. 2 indicates the results of EIT when α equals 1, 0.1, 0.01, 0.005, 0.003236, 0.003233, and 0.003231, respectively. EIT can be used to reconstruct an overall image in any case with low resolution at the boundaries of the lung and heart. For larger α values, smoother images are obtained. The second and third rows are the results of CEIT when we fix β and choose different α. The boundaries of the objects are sharp and precise. In addition, when α is set to 0.003231, the

result from EIT is distorted due to issues related to singular values. However, CEIT can provide a stable solution due to the cross-gradient constraints. The images in the fourth row show the results of a fixed α and varying β. If β is too small, the cross-gradient term cannot constrain the EIT image. If β is too large, the voltage data misfit cannot be reduced to a sufficiently small value, and the reconstructed model is inaccurate.

Shape errors

In practical applications of CEIT method, the synchronous acquisition of CT and electrical measurement data may be challenging since human respiration or movement may cause inconsistent structural information between CT images and conductivity distributions.

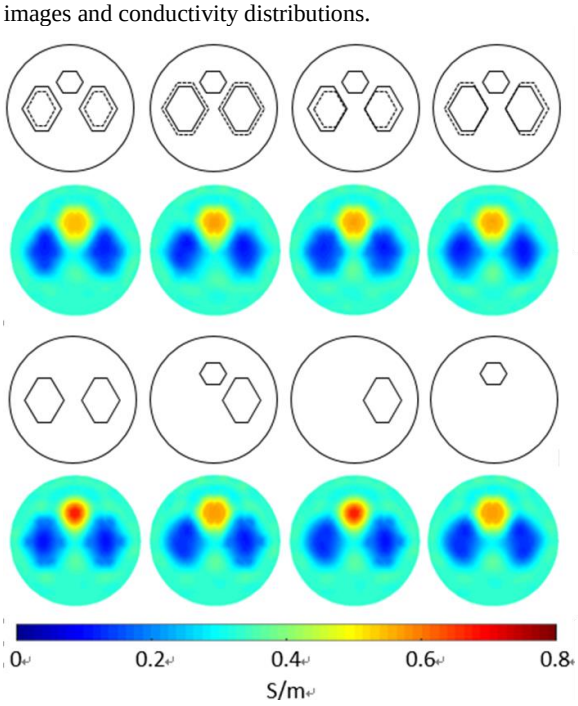

Fig 3: Image reconstructions (Cases 1–8) with CT scans obtained from human respiration or movement (top), and incomplete structure descriptions (bottom).

It is also difficult for the CT image to represent the entirety of the interior structures in the human body. For example, the CT value of a human heart is usually close to the soft tissue, and pleural effusion can also result in similar CT values between the lungs and soft tissue. We set α and β to 10^{-3} and 1, respectively, for CEIT. Four reconstruction images, corresponding to Cases 1–4, obtained by CEIT along with the model errors in the CT-scans caused by human respiration or movement are shown in the first and second rows, respectively, of Fig. 3. The third and fourth rows denote the results from Cases 5–8 by CEIT along with the model errors resulting from incomplete structure descriptions. The dashed lines in the plots denote the boundary changes from a 'perfect' CT scan to one with model errors. The results suggest acceptable variations to the model errors caused by the incomplete structure descriptions.

We also consider another two models with simulated pathologies depicted in Fig. 4: an injured thorax (Case 1) and a pleural effusion (Case 2). For both scenarios, the conductivities of the heart, lungs and background are set to 0.6 S/m, 0.15 S/m, and 0.33 S/m, respectively, and the corresponding CT values are set to -700 HU, 60 HU, and 30 HU, respectively. The lung injury region and background medium are assumed to have the same conductivities and CT values. The conductivity of the pleural effusion is 0.6 S/m with the same CT value as the background. The recording geometry and the numerical solutions for the forward problems are similar to those in section III. The forward calculations apply a piecewise constant model with a mesh of 2,773 triangular elements and 1,348 nodes. A mesh of 1,385 elements and 737 nodes is used in the inversion problem. A homogeneous conductivity model with σ_0 = 0.33 S/m is employed for both EIT and CEIT as the starting model.

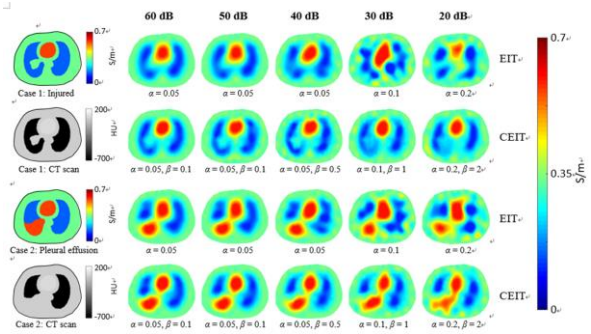

Fig 4: Reconstructions of injured and pleural effusion examples from noisy numerical tests.

Case 1: Simulated injured lung: we obtain the results of conventional EIT and CEIT using the same regularization factor for each noise level. The regularization parameter α and cross-gradient parameter β are gradually increased for handling with the decreasing SNR. The final data misfit of the two methods is close at each noise level. We conclude that in the case of a high SNR, conventional EIT can reconstruct a reasonable image but produces low resolution in the injured area, where CEIT is able to produce a clear image. When the SNR drops to a low value such as 30 dB or 20 dB, conventional EIT can no longer resolve a reliable solution, and the quantitative indicators are increased. However, CEIT can mitigate the distortions from a low SNR due to the use of cross-gradient constraints. The

variations in the model misfit, WD, and DT of CEIT are accordingly stable as the SNR decreases. In medical imaging, the shape indicators widening (WD) and distortion (DT) are often used to evaluate the imaging results.

Case 2: Simulated pleural effusion*:* this test is designed for situations involving incomplete structures in the referenced CT scan. The pleural effusion is designed to be undetected in the CT scan. The parameter selections are similar to those of Case 1. As we concluded for Case 1, the reconstructed images of EIT are distorted due to the low SNR. The areas detected in the referenced CT scan are well reconstructed by CEIT, and the evolution of average quantitative indicators also indicates well reconstructed images of CEIT with respect to the different SNR. Nevertheless, at the low SNRs, the reconstructions of CEIT for the pleural effusion are distorted due to the lack of cross-gradient constraints in this area.

Phantom experiments

To demonstrate the efficacy of the proposed approach, we utilize the experimental data that were applied in (Liu et al., 2017).

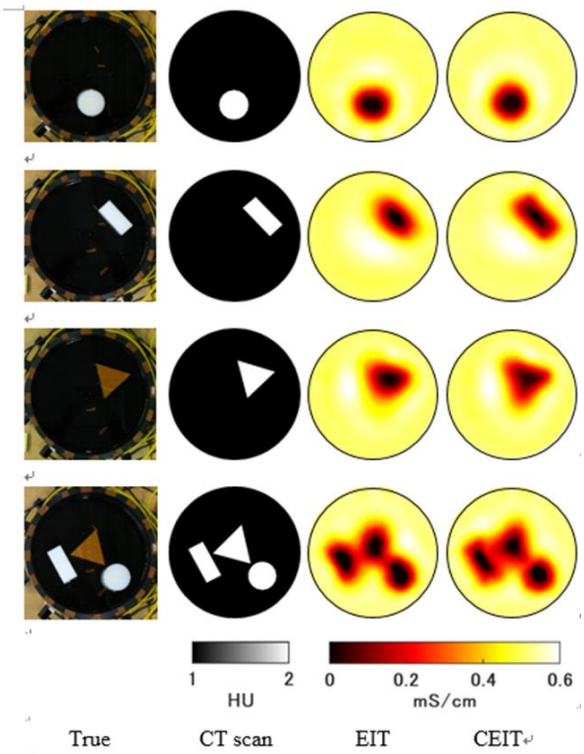

Fig.5: Reconstructions of phantom experiments with both EIT and CEIT methods. Inclusions are composed of plastic objects. Cases 1–4 are shown from top to bottom.

The experiments consist of four different cases (left column of Fig. 5) involving the plastic objects (insulators) with different shapes inserted into a tank. These physical models and data serve as a step forward from numerical model testing, an approach commonly applied in developing and testing any new medical imaging technique.

In these experiments, the conductivity of the background (saline) is measured as 543 μS/cm. Because CT measurements are unavailable for the experiments, we simulated approximate CT scan images with 1 HU for saline and 2 HU for the plastic objects in each case, and note that the cross-gradient method mainly utilizes the structure information in the domain of the scan. The contact impedance is measured as 1×10^{-4} $\Omega\cdot m^2$ for all electrodes. The tank data are acquired from the KIT4 recording geometry as described above. The injected current is set to 1 mA with a frequency of 10 kHz. A FEM is applied to numerically approximate a CEM model for forward modeling. The forward and inversion grids applied in this analysis are the same as those used for the simulation of the blocky model. A homogeneous conductivity model with σ_0 = 0.57 mS/cm is employed as the starting model in all cases.

The imaging results of Cases 1–4 from EIT and CEIT are shown in Fig. 5. As we can see, EIT reconstructs a reasonable image of the inclusions but with relatively low resolution at the boundaries. The details of the inclusions, especially the sharp edges, are barely distinguished in the images from EIT. Due to the CT image constraints, CEIT reconstructs the targets with improved resolution, recovering the shape of the targets more accurately, and the conductivity contrast is enhanced near the edges of the inclusions.

Conclusions

Similar to joint geophysical imaging, the cross-gradient method serves as a link between different medical imaging methods for the same reconstructed target. A CT image-guided electrical impedance tomography method is proposed and tested in this study. CEIT is evaluated by comparing with EIT in both simulations and phantom experiments. The results prove that CT information can be applied to EIT by utilizing the cross-gradient method, thereby providing high resolution images. The simulations of thorax geometry models show that the CEIT method is robust against noise. The further potential of this study is to apply the cross-gradient function to the combinations of different medical imaging methods.

Acknowledgments

The authors would like to thank the inverse problem group at the University of Eastern Finland (UEF), for providing us with the experimental data.